

Review

Morphological Control Agent in Ternary Blend Bulk Heterojunction Solar Cells

Hsueh-Chung Liao^{1,2,3}, Po-Hsuen Chen^{1,4}, Robert P. H. Chang² and Wei-Fang Su^{1,*}

¹ Department of Materials Science and Engineering, National Taiwan University, Taipei 106-17, Taiwan; E-Mails: hcliao@northwestern.edu (H.-C.L.); grimace050101@gmail.com (P.-H.C.)

² Materials Science and Engineering, Northwestern University, Evanston, IL 60208, USA; E-Mail: r-chang@northwestern.edu

³ FrontMaterials Co. Ltd., New Taipei City 23441, Taiwan

⁴ Materials Science and Engineering, Illinois Institute of Technology, Chicago, IL 60616, USA

* Author to whom correspondence should be addressed; E-Mail: suwf@ntu.edu.tw; Tel./Fax: +886-2-3366-4078.

External Editor: Alexander Böker

Received: 15 September 2014; in revised form: 16 October 2014 / Accepted: 23 October 2014 /

Published: 3 November 2014

Abstract: Bulk heterojunction (BHJ) organic photovoltaic (OPV) promise low cost solar energy and have caused an explosive increase in investigations during the last decade. Control over the 3D morphology of BHJ blend films in various length scales is one of the pillars accounting for the significant advance of OPV performance recently. In this contribution, we focus on the strategy of incorporating an additive into BHJ blend films as a morphological control agent, *i.e.*, ternary blend system. This strategy has shown to be effective in tailoring the morphology of BHJ through different inter- and intra-molecular interactions. We systematically review the morphological observations and associated mechanisms with respect to various kinds of additives, *i.e.*, polymers, small molecules and inorganic nanoparticles. We organize the effects of morphological control (compatibilization, stabilization, *etc.*) and provide general guidelines for rational molecular design for additives toward high efficiency and high stability organic solar cells.

Keywords: organic solar cell; bulk heterojunction; additive; morphology; ternary blend system

1. Introduction

Organic photovoltaics (OPVs) have attracted considerable research interests and shown significant progress over the past two decades. The advantages of low-cost, solution processibility, semi-transparency, mechanical flexibility, light weight, *etc.* promise the integration with a variety of products, e.g., portable electronics, buildings, accessories, *etc.* Achieving high power conversion efficiency (PCE) of OPV devices to align with conventional inorganic photovoltaic (PV) systems is the main goal of investigation. Nonetheless, the OPVs are generally suffered from the low dielectric constant of organic materials, which results in short exciton diffusion length (~10–20 nm) and low efficient exciton dissociation and carrier transport itself. Apparently, the planar heterojunction in which the carriers/excitons are required to transport throughout the spatially separated layer (typically 100–300 nm) is not suitable for OPV. A remarkable breakthrough is the implement of bulk heterojunction (BHJ), which is comprised of inter-penetrated p-type (electron donor, e.g., conjugated polymers) and n-type (electron acceptor, e.g., fullerene derivatives) organic materials. The two materials constitute p–n junction for exciton dissociation at the interfaces and bi-continuous phases for carrier transport toward respective electrodes. The introduction of BHJ overcomes the inherent limitation of organic semiconductors. Therefore, the BHJ solar cell to date holds the leading PCE values of OPV system around 7%–11% in lab-scale and takes the majority of OPV studies [1]. Some important subjects regarding the advance of OPV over the past decades can be referred to the comprehensive review articles, *i.e.*, materials development [2–5], morphology [1,6–10], device physics [11–14], device structure [15].

How to control the three-dimensional nanomorphology of BHJ film has never been trivial and has become one of the crucial subjects of investigation. Various strategies have been reported to tailor the morphology from local-scale (molecular ordering/conformation) to global-scale (domains/networks in tens and hundreds of nanometer) e.g., thermal annealing [16–19], solvent vapor annealing [17,20], type of processing solvents [21], incorporation with solvent additives [1,22], *etc.* These morphological control methods and associated characterization techniques have also been comprehensively reviewed [1,6–10,23,24]. In our previous review article, we systematically summarized the effects of incorporating solvent additives which has found to be effective in a variety of BHJ systems [1]. In short, the solvent additives function to control the film-drying rate and differentiate the solubility of BHJ materials from host solvents. It is noteworthy that those additives are generally regarded as processing solvents, which evaporates with film-drying.

The concept of ternary blend attracted a great deal of attentions in last five years [25–27]. It was mainly proposed to address the limitation of narrow absorption width within the solar spectra (typically in visible light region) by single BHJ devices. Most of the researches focused on extending the energy conversion to near-infrared region through three different mechanisms: *i.e.*, charge transfer, energy transfer or parallel-linkage [27]. Interestingly, it was discovered that the introduction of the third (or more) component assists to optimize and stabilize the BHJ blends. Recently, more and more researches demonstrated that the BHJ morphology can be controlled by including additives. In this contribution, we review the effects of incorporating additives as morphological control agents in polymer-based BHJ solar cells. The additive together with main donors (*i.e.*, polymer) and acceptors (*i.e.*, fullerene derivatives) constitute a ternary blend which is distinctive to our previous review work

emphasizing on processing solvent additives [1]. The promising candidates for morphological control agents can be polymers, small molecules, inorganic nanoparticles, *etc.* It is noteworthy that beside the ternary components, the solvents used for solution processing would residue in the BHJ films [28], especially the solvents with high boiling points. This leads to the thin film in reality multi-components system. For clarification, herein the binary or ternary systems refer to the number of solid-state components in BHJ thin films.

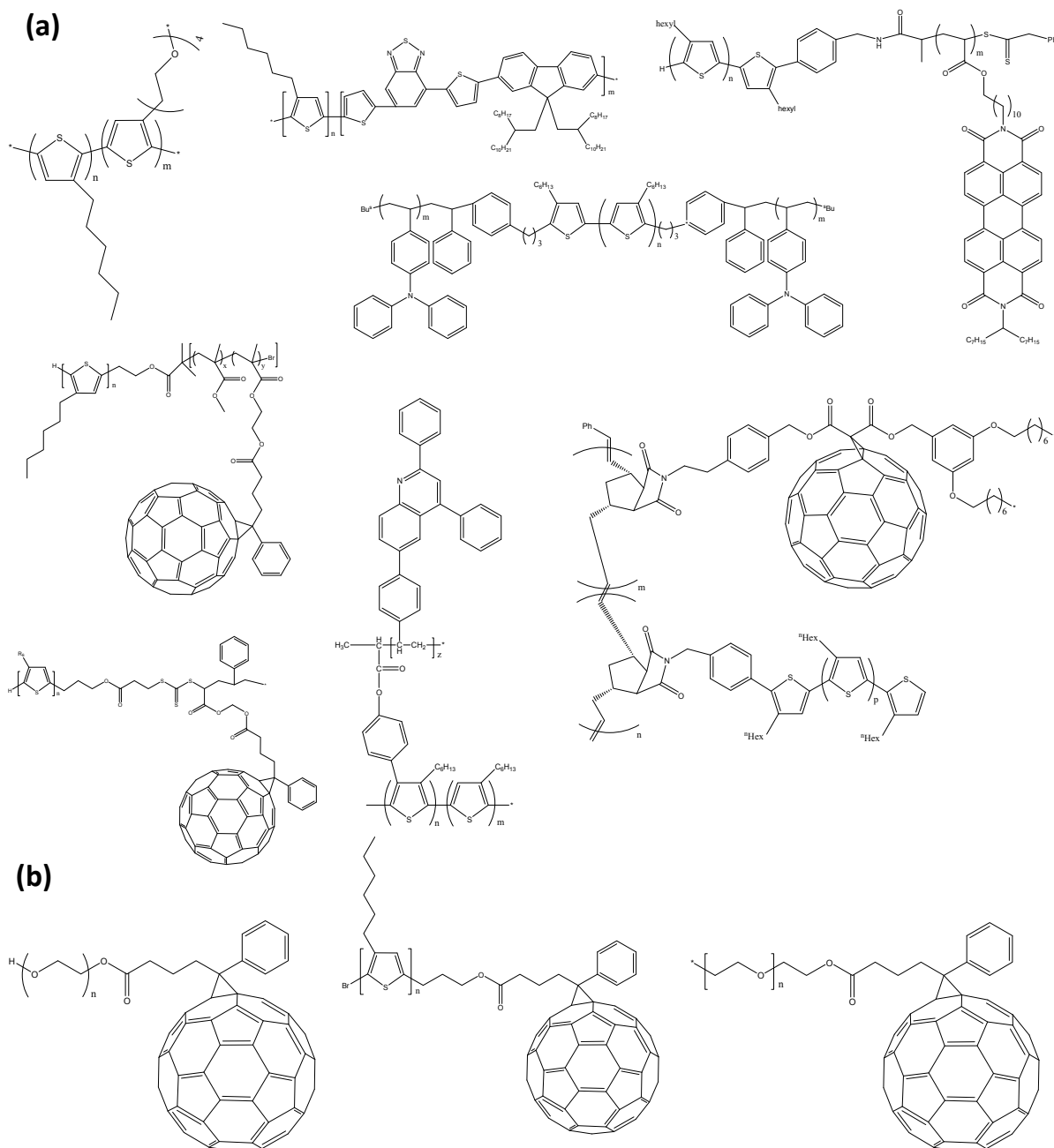
2. Polymers

Considering the exciton diffusion length of ~10–20 nm in organic semiconductors, a general picture of optimized morphology is comprised of phase-separated domains of donors (e.g., conjugated polymers) and acceptors (e.g., fullerene or its derivatives) in tens of nanometers. This provides sufficient interface areas for exciton dissociation and bi-continuous percolated networks for carrier transport. The miscibility between donors and acceptors is hence vital in dominating the BHJ morphology. Specifically, weak miscibility between donors and acceptors leads to severe phase segregation (up to sub-micron or micro-scale), which is detrimental to device performance. In the early development of OPVs (early 21st century), because of the weak miscibility between fullerene and conjugated polymers, two major strategies were proposed to conquer the challenge. From the chemical aspect, researches devoted much effort to chemically modifying the fullerene molecules in order to enhancing their solubility and compatibility with conjugated polymers. Meanwhile, the other alternative strategy was to include a compatibilizer into BHJ (ternary blend) [29–31]. It was reported that by embedding conjugated polymers and fullerene C₆₀ into plastic polymer matrix such as polystyrene (PS), polyvinylcarbazole (PVK), *etc.*, the homogeneity of the thin films could be improved [29–31]. Disappointedly, the photovoltaic properties were deteriorated due to the insulating matrix. Even though the invention of fullerene derivatives: [6,6]phenyl C₆₁-butyric acid methyl ester (PC₆₁BM), *i.e.*, chemical modification method, has solved the compatibility problem during film forming processes, the BHJ morphology is still thermally unstable. Severe segregations were still observed after the BHJ films were thermally annealed at high temperature or for long time. Therefore, the additive strategy still plays an important role in morphological control aspect of BHJ film in solar cell.

2.1. Copolymer

Copolymers became one of the promising compatibilization candidates, especially well-defined di-block copolymer [32,33]. They typically reveal unique self-assembly nanostructures and semiconducting characteristics [32–36]. Various kinds of copolymers were designed, synthesized and incorporated into BHJ with remarkable PCE improvements and/or PCE preservation. Their chemical structures are representatively shown in Figure 1a.

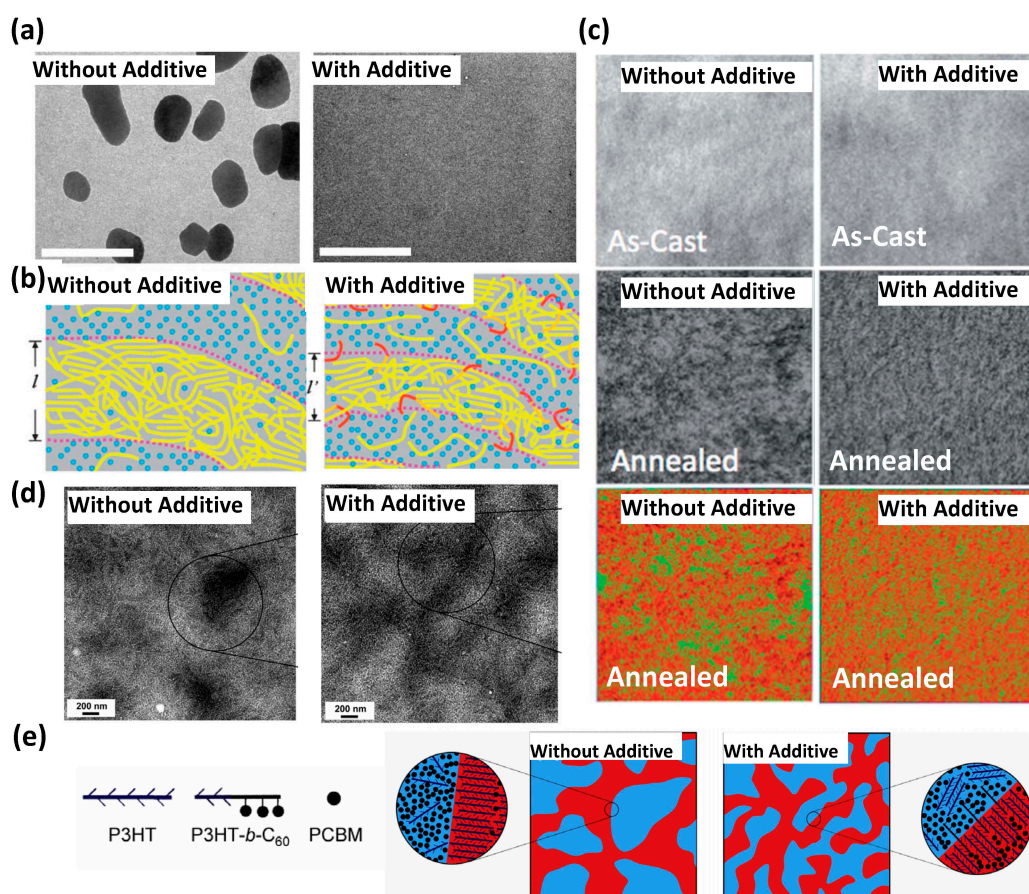
Figure 1. Representative (a) copolymers and (b) homopolymers as morphological control agents. Reprinted with permission from [37] copyright 2010 American Chemical Society; from [38] copyright 2006 Wiley; [39] copyright 2009 Royal Society; [40] copyright 2010 IOP Science; [41] copyright 2013 Elsevier; [42–44] copyright 2011, 2009, 2007 American Chemical Society; [45] copyright 2011 Wiley; [46,47] copyright 2011, 2010 Royal Society.



In 2006, Sivula *et al.* included a di-block copolymer containing poly(3-hexylthiophene) (P3HT) macromonomer and fullerene into P3HT/PC₆₁BM BHJ blends [38]. The photovoltaic performances were not degraded in the ternary blends. Moreover, the incorporated diblock copolymer effectively prevented the segregation of micro-sized P3HT and PC₆₁BM domains against destructive long-time thermal treatment (Figure 2a). The diblock copolymer can be regarded as a morphological stabilizer, which lowered down the surface energy (surface tension) between P3HT and PC₆₁BM.

Subsequently, a morphological investigation was reported by Chen *et al.* who emphasized on the manipulation of nano-scaled domains structure of P3HT/PCBM/P3HT-*b*-poly(ethylene oxide) (P3HT-*b*-PEO) ternary blends by including the rod-coil diblock copolymer additive P3HT-*b*-PEO [48]. The PEO segments could interact with PC₆₁BM and situate at P3HT/PC₆₁BM interfaces as illustrated in Figure 2b, thereby driving self-assembled nanostructures. As shown in Figure 2c of the energy-filtered TEM images, the thermally annealed ternary blend films (incorporating concentration of 5%–10%) distinctively show nanofibril nanostructures as compared to the binary film, while their morphologies in the as-casted film are similar. The authors performed the grey value analysis to quantitatively estimate the P3HT domain sizes. It showed the P3HT domains were reduced to 14 ± 3 nm and 10 ± 2 nm for 5% and 10% P3HT-*b*-PEO doping concentrations respectively as compared to the binary blends of 17 ± 3 nm.

Figure 2. (a) TEM (Transmission electron microscope) images of P3HT/PC₆₁BM with and without 17 wt% diblock copolymer. The scale bar is 2 μ m; (b) Illustration of P3HT/PC₆₁BM without and with 10% additive P3HT-*b*-PEO; (c) P3HT mapping obtained from energy filtered TEM images before (top) and after (middle) thermal annealing for P3HT/PC₆₁BM blend films without and with 10% P3HT-*b*-PEO respectively. The bottom row images are the color-scaled middle row images in which the green color represents the P3HT-rich domains; (d) TEM images of P3HT/PC₆₁BM blend films without and with 2.5% P3HT-*b*-C₆₀ additive; and (e) Schematic representations of P3HT/PC₆₁BM blend films without and with P3HT-*b*-C₆₀ additive. Reprinted with permission from [38] copyright 2006 Wiley; [40] copyright 2010 IOP Science; [48] copyright 2012 Royal Society.



Lee *et al.* developed a P3HT-*b*-C₆₀ diblock copolymer with C₆₀ unit attached on the coil part and also thoroughly investigated the morphological evolution compatibilized and stabilized by the additive [40]. The TEM (Transmission electron microscope) observations of P3HT/PC₆₁BM blend after long-time thermal annealing clearly revealed aggregated P3HT and PC₆₁BM domains (Figure 2d) with respective crystallites. In contrast, weaker contrast was observed in the ternary blends with P3HT-*b*-C₆₀ additives, which implied the better miscibility and inter-penetration. The authors pointed out the effects of additives situated at P3HT/PC₆₁BM interfaces: (1) reduce surface tension for the binary phases and (2) kinetically lower the rate of aggregation, as schematically illustrated in Figure 2e.

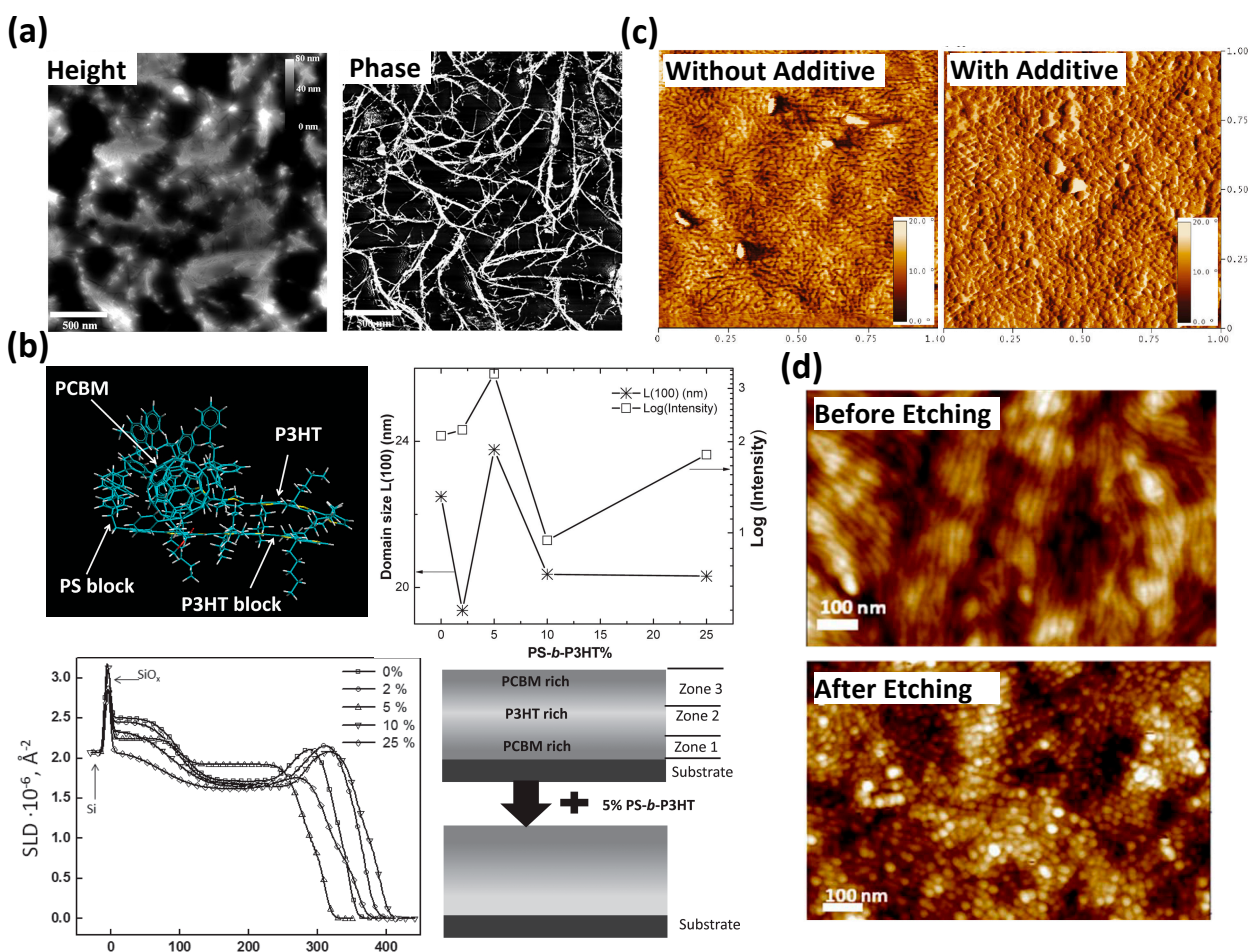
The articles reviewed above mainly focused on the effect of morphological stabilization against thermal treatment. The PCEs of the ternary blends they showed were similar or slightly reduced as compared with the reference binary blends. It can be attributed to the insulating segment of copolymers, which impeded the carrier transport throughout the films. Therefore, as a morphological control agent the design and control over the chemical structure and conformation of copolymer is extremely critical to achieve a more advanced goal: improve device performance by optimizing BHJ morphology.

In 2009, Yang *et al.* synthesized a (P3HT-*b*-P(SxAy)-C₆₀) with exclusive nanofibers structure (Figure 3a) which showed effectiveness on P3HT/PC₆₁BM morphological control with enhanced PCEs by 30% [39]. Subsequently, Sun *et al.* utilized 5 wt% copolymer additive polystyrene-*block*-poly(3-hexylthiophene) (PS-*b*-P3HT) to obtain favorable BHJ morphology with increased PCEs from 3.3% to 4.1% [49]. The authors elucidated that the additive-induced morphology was resulted from the interaction of PS segment with PC₆₁BM phase and P3HT block with P3HT phase as shown in Figure 3b. Such interaction led to higher P3HT crystallinity (long range order) that facilitated carrier transport as shown in Figure 3b of the structural parameters extracted from grazing incidence X-ray diffraction (GIXD) results. Furthermore, it also attributed to the PC₆₁BM diffusion toward favorable distribution along the vertical direction, which was clearly revealed by neutron reflectivity (NR) characterizations (Figure 3b). The highest PCEs of 4.4% for P3HT/PC₆₁BM/copolymer ternary blends was reported by Tsai *et al.* who designed and synthesized a coil-rod-coil tri-block copolymer: poly(4-vinyltriphenylamine)-*b*-poly(3-hexylthiophene)-*b*-poly(4-vinyltriphenylamin) (PTPA-P3HT-PTPA) with self-assemble periodic lamellar structure of 10–12 nm [37]. The high efficiency was resulted from the additive-induced sphere-like nanostructure (Figure 3c) for enhancing donor/acceptor interface area. The PTPA segments preferred to interact with PC₆₁BM, which suppressed the PC₆₁BM aggregation during thermal annealing and remains the ordered P3HT crystal structure. Therefore, from the literature, copolymers as morphological control agents can, not only contribute to morphological stabilization, but also optimization.

The polymer-polymer BHJ systems were proposed to address the stability issue of fullerene derivatives as acceptor. However, the thermodynamically driven phase-separation in micron-scale limited the progress of device performance. Similar to the cases reviewed above, a compatibilizing copolymer composed of the molecular structures of both donor and acceptor can be used to bridge the binary phases and control the phase-separated morphology in nanoscale. Mulherin *et al.* synthesized an all-conjugated diblock copolymer poly(3-hexylthiophene)-*block*-poly[2,7-(9,9-dialkyl-fluorene)-*alt*-5,5-(4',7'-di-2-thienyl-2',1',3'-benzothiadiazole)] (P3HT-*b*-PFTBTT) for mediating the P3HT/PFTBTT polymer-polymer blend BHJ [42]. The copolymer was discovered to suppress the phase separation along lateral direction while remain the crystallization of P3HT along the vertical direction [42].

Furthermore, the standing lamellar structure with size of 25 nm was induced by the copolymer inside the thin film (Figure 3d), which is comparable to exciton diffusion length and facilitates charge transport.

Figure 3. (a) Height and phase images of pristine P3HT-*b*-P(SxAy)-C₆₀ with exclusive nanofibers structure; (b) P3HT/PC₆₁BM morphology tuned by 5 wt% copolymer additive PS-*b*-P3HT in vertical and horizontal direction. The left-top is the density functional theory (DFT) calculations revealing the interaction of PS-*b*-P3HT with P3HT and PCBM. The right-top is the summarization of structural parameters of P3HT crystallites extracted from GIXD results. The left-bottom is the scattering length density profile obtained from NR fitting and the corresponding concentration distribution is illustrated in the left-right figure; (c) AFM (Atomic force microscope) images of P3HT/PC₆₁BM blend films without and with 1.5% PTPA-P3HT-PTPA additive; and (d) AFM images of ternary film surface with additives P3HT-*b*-PFTBTT before and after the removal of top 10 nm surface layer by etching. Reprinted with permission from [37] copyright 2010 American Chemical Society; [39] copyright 2009 Royal Society; [42] copyright 2011 American Chemical Society; [49] copyright 2011 Willey.

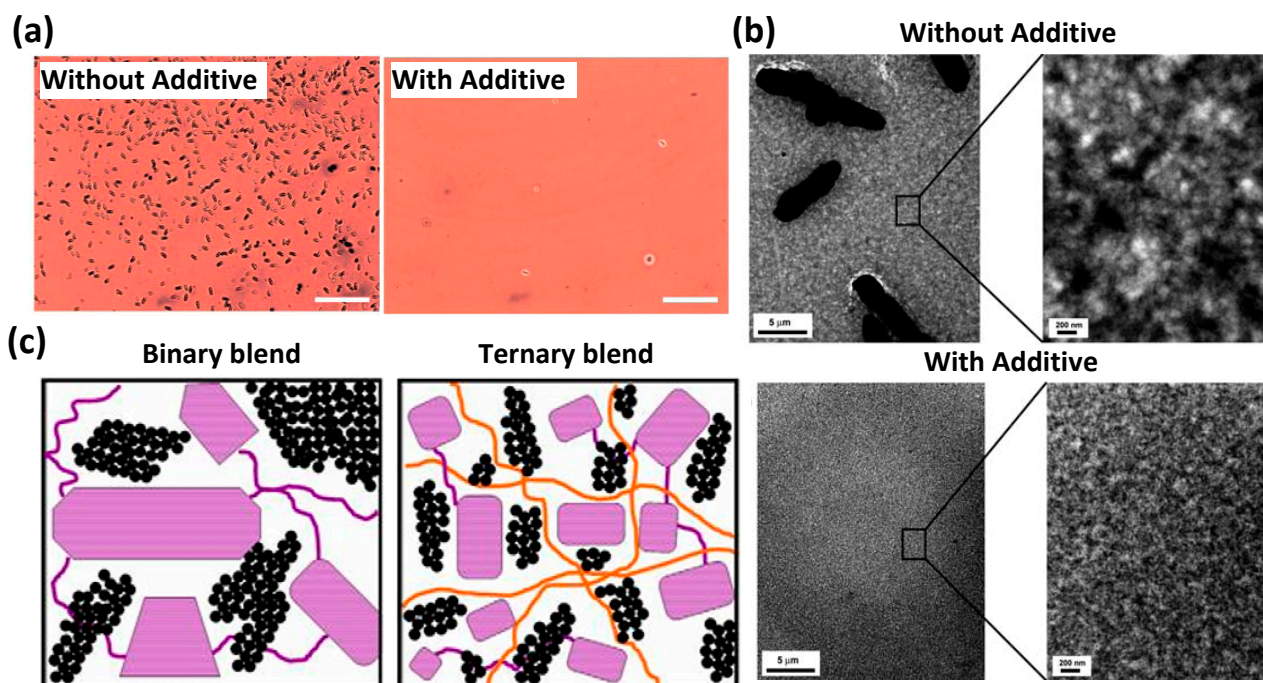


2.2. Homopolymer

There were some references adopted homopolymers, which also revealed capability in BHJ morphological control. They are generally designed to bear the moiety of both host donors and

acceptors for mediating in between. Their chemical structures are selectively shown in Figure 1b. Tai *et al.* developed a fullerene end-capped polyethylene glycol which was doped in P3HT/PC₆₁BM BHJ device as an additive [46]. The Fourier transform infrared spectroscopy (FTIR) provided the evidence that the additives uniformly distributed within the BHJ film in which the immobile end C₆₀ cages served as the nucleation sites for PC₆₁BM crystallization. The uniformly distributed and static PC₆₁BM crystallites with size of several nanometers attributed to the considerably improved device performance and morphological stability after thermal aging at 60 °C for 300 h (Figure 4a). Similar effects were presented by Lee *et al.* using C₆₀-end capped P3HT as stabilizer to preserve around 70% of the original PCE after 200 h thermal annealing at 100 °C (Figure 4b) [47]. Campoy-Quiles reported the ternary blend of region-random P3HT, region-regular P3HT and PC₆₁BM in which the region-random P3HT defined domains (scaffolds) were comprised of soft polymer chains [50]. The glassy entanglements of amorphous polymer chains assisted to stabilize the morphology and enhanced the P3HT crystallinity with larger number of crystallites but smaller crystal size. Consequently, increased V_{oc} and PCE can be attained due to the morphology-induced energy level shift.

Figure 4. (a) Optical microscopy images of P3HT/PCBM BHJ without and with additives fullerene end-capped polyethylene glycol after thermal aging at 60 °C for 300 h; (b) TEM images of P3HT/PCBM BHJ without and with additives C₆₀-end capped P3HT after thermal aging at 150 °C for 48 h; (c) Schematic illustrations of P3HT:regular/PCBM binary blend and P3HT:regular/P3HT:random/PCBM ternary blend. Reprinted with permission from [46,47] copyright 2011, 2010 Royal Society; [48] copyright 2012 Elsevier.



Homopolymer was also found to be capable of tuning the morphology of other BHJ systems. The poly[2,6-(4,4-bis-(2-ethylhexyl)-4H-cyclopenta[2,1-b;3,4-b']dithiophene)-alt-4,7(2,1,3-benzothiadiazole)] (PCPDTBT) has been a popular low-band gap conjugated copolymer since the first introduction in 2007 [22–24]. However, it has low tendency to organize into ordered crystalline when blended with

acceptor [6,6]-phenyl C₇₁-butyric acid methyl ester (PC₇₁BM) [25]. The most widely adopted strategy is processing with solvent additives [22,51]. In 2013, Chang *et al.* demonstrated the inclusion of crystalline P3HT as a morphological control agent into PCPDTBT/PC₇₁BM BHJ solar cell for further improving the device performance [52]. The 1 wt% P3HT benefited the crystallinity (π - π staking) of P3HT and phase separation of PCPDTBT/PC₇₁BM. The favorable morphology in ternary system enhanced the charge transport and the PCE by 17%.

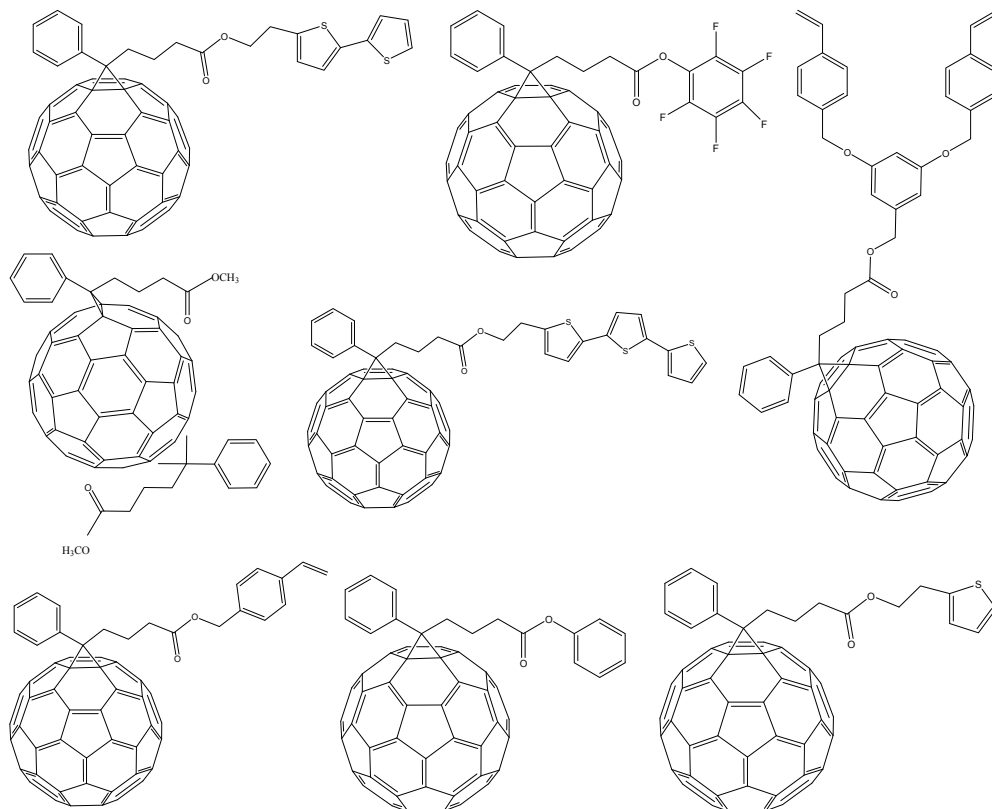
To sum up, for rationally designing a good polymer as a morphological compatibilizer and/or stabilizer, the following criteria can be served as rational guides for additive design/selection: (1) one of the segments would interact with the PCBM phase so that the additive is able to hinder the PCBM segregation against thermal treatment; (2) the additive would prefer to situate at donor/acceptor interfaces for reducing the surface tension (energy); (3) the additive itself would possess self-assemble nanostructures (especially for the copolymers including insulating parts) for preventing from impeding carrier transport; (4) the additive would not suppress, or even more can help the organization of host polymers and acceptors into crystalline structures.

3. Small Molecules

Small organic molecules can be also served as morphological control agents with careful chemical design and synthesis. Among these additives, the fullerene derivatives take the majority due to its compatibility with host acceptors as well as the established solvent systems, though there were other small molecules that revealed a similar function [53–55]. Herein we focus on the development of a variety of kinds of fullerene derivatives as morphological control agents.

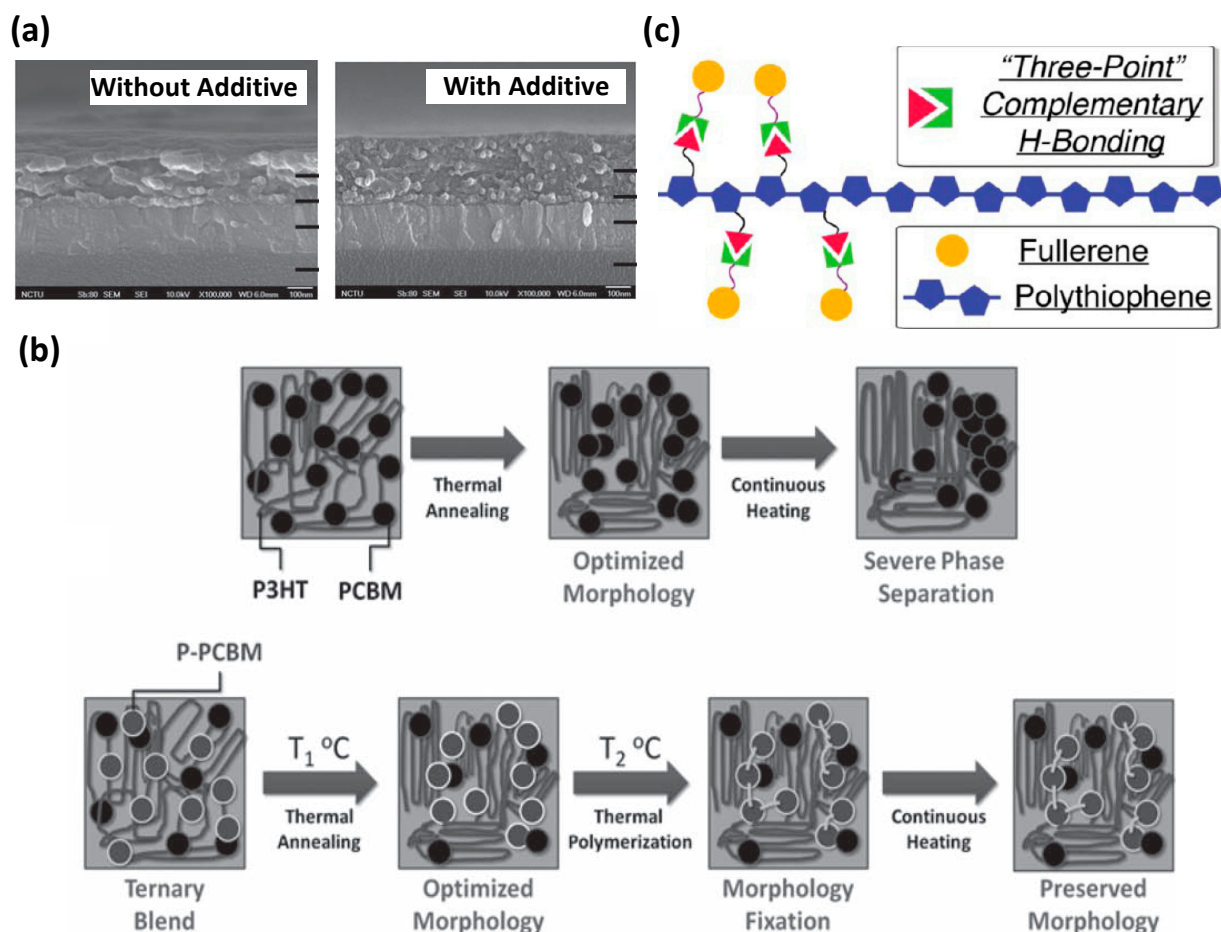
Since the ultrafast injection of electron from conjugated polymers to fullerene derivatives was discovered, they have been the most popular acceptor materials [56]. The PC₆₁BM or PC₇₁BM, particularly, attracted an explosion of investigations and were generally used in various BHJ solar cell systems. However, there are some obstacles of PC₆₁BM or PC₇₁BM needed to be addressed: (1) their energy level leads to low V_{oc} when paired with typical semiconducting polymers; (2) they are typically thermal unstable and tend to diffuse to form large-scaled aggregation under destructive thermal treatment. Hence, recently the development of alternative derivatives has been extensively studied and shown significant progress [57]. Even though the highest efficiencies (single junction cell) in academic articles were still based on PC₇₁BM [1], some of the fullerene derivatives have shown their unique properties in influencing the morphology of BHJ blends. Therefore, adding these fullerene derivatives (representatively shown in Figure 5) into high efficiency polymer/PC₆₀BM (*i.e.*, ternary blend) promises the goal of further improving device performances and stability.

Figure 5. Representative fullerene derivatives as morphological control agents. Reprinted with permission from [58] copyright 2012 Elsevier; [59,60] copyright 2011, 2014 Wiley; from [61] copyright 2012 Royal Society.



In 2011, Cheng *et al.* synthesized two crosslinkable fullerene derivatives: styryl-functionalized, [6,6]-phenyl- C_{61} -butyric acid styryl dendron ester (PCBSD) and [6,6]-phenyl- C_{61} -butyric acid styryl ester (PCBS) which were doped into P3HT/ $PC_{61}BM$ BHJ blends respectively [59]. The *in situ* crosslinking of fullerene derivatives through styrene groups effectively fixed the morphology with phase-separated domains in nanoscale after long-time thermal annealing (150 °C for 25 h) while the P3HT/ $PC_{61}BM$ binary blends revealed severe phase segregation as shown in the SEM (scanning electron microscope) images (Figure 6a) and schematic illustrations (Figure 6b). The corresponding solar cells respectively showed a steady PCE of 3.8% and dramatically degraded PCEs of 0.69% after such isothermal annealing. Instead of using covalent bonding, Li *et al.* prepared a ternary blend: polythiophene diblock copolymer (P4)/ $PC_{61}BM$ /diaminopyridine tethered fullerene derivative (PCBP) and studied the self-assembly between P4 and PCBP [62]. The authors proposed that these two components formed a strong complex through “three point” complementary hydrogen bonding between diaminopyrimidine and thymine moieties (Figure 6c). The morphologies of the ternary blend films can be hence tunable toward long-range order with improved device performance and stability.

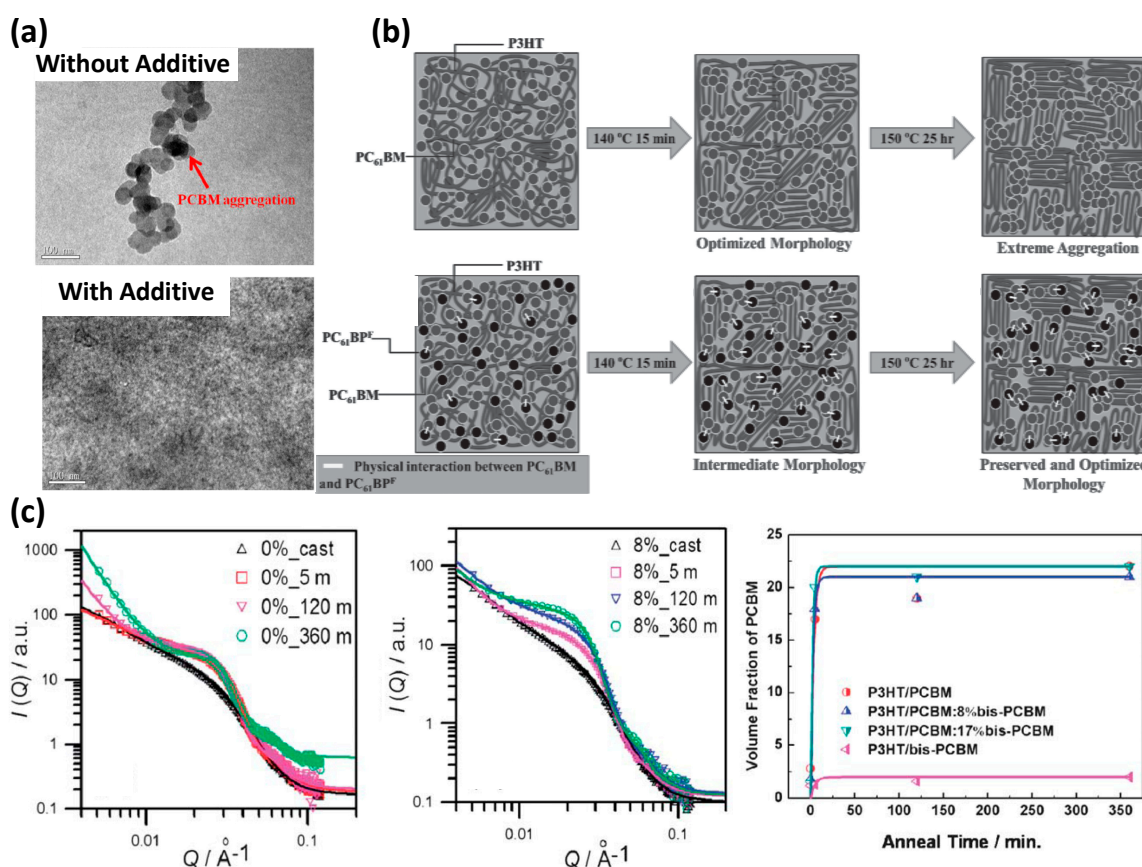
Figure 6. (a) SEM cross-sectional images of P3HT/PCBM solar cell device without and with additive: crosslinkable fullerene derivatives, after thermal annealing at 150 °C for 25 h; (b) Schematic illustration of the P3HT/PCBM morphological evolutions without and with additives: crosslinkable fullerene derivatives, respectively under thermal treatments and thermal aging; (c) Illustration of three-point hydrogen bonding among polythiophene, fullerene and additive. Reprinted with permission from [59] copyright 2011 Wiley; [62] copyright 2013 American Chemical Society.



In addition to covalent and hydrogen interactions, several work reported the morphological control through physical interactions (e.g., stereo hindrance, surface energy, *etc.*) among additives and host BHJ materials. Lai *et al.* synthesized a series of fullerene derivatives with various thiophene units as surfactants [58]. Mediated by the designed oligothiophene-fullerene derivatives, they helped the organization of P3HT phase and constrained the PC₆₁BM diffusions by reducing the P3HT/PC₆₁BM surface energy (Figure 7a). It efficiently led to remarkably improved PCE up to 4.37% and little loss after thermal annealing test at 150 °C for 10 h. Similar effects were discovered by Liao *et al.* who developed fullerene derivative: [6,6]phenyl-C₆₁ butyric acid pentafluorophenyl (PC₆₁BPF) bearing pentafluorophenyl group [60]. The pentafluorophenyl group with the PC₆₁BM cages formed a supermolecule, which imparted restriction to the thermal-driven diffusion during thermal aging (Figure 7b). The author furthermore pointed out that morphological stabilization by PC₆₁BPF promised the universal application to other low band-gap conjugated copolymer/fullerene systems, e.g.,

poly(dithienobenzocarbazole-*alt*-dithienylbenzothiadiazole) (PDTBCDTBT)/PC₇₁BM which showed a 81% of original PCEs after isothermal heating at 150 °C for 25 h. Liu *et al.* used *bis*-adduct of PC₆₁BM (*bis*-PC₆₁BM) to inhibit the formation of large PC₆₁BM clusters and retain the sufficient donor/acceptor interfaces [61]. Taking *bis*-PC₆₁BM as the additive benefited the ease of solvent selection and prevented extra synthesis procedure since it is a byproduct of PC₆₁BM. By adding 8.3 wt% of *bis*-PC₆₁BM, the devices showed enhanced performance from 3.09% of reference cell to 3.62% with extremely high thermal stability.

Figure 7. (a) TEM images of P3HT/PCBM blends without and with additive [6,6]-phenyl-C₆₁-butyric acid 2-(2',2'':5'',2''-terthiophene-5'-yl)ethyl ester (PCBTTE) under 150 °C for 10 h; (b) Schematic illustration of the P3HT/PCBM morphological evolution without and with PC₆₁BPF additives respectively under thermal treatments and thermal aging; (c) GISAXS (small angle X-ray scattering) profiles of as-casted and thermally annealed P3HT/PCBM for 5, 120, and 360 min respectively without and with 8% *bis*-PCBM. The right figure summarizes the volume fraction of PCBM clusters (extracted from GISAXS profiles) during thermal aging. Reprinted with permission from [58] copyright 2012 Elsevier; [60] copyright 2014 Wiley; [63] copyright 2013 American Chemical Society.



This work was subsequently investigated by employing powerful grazing incidence wide/small angle X-ray scattering (GIWAXS/GISXAS) technique (Figure 7c) to explore the morphological evolutions and mechanisms in which the findings beyond the knowledge at that time were pointed out [63]. The GIWAXS/GISAXS technique with modeling has been intensively utilized to quantitatively

characterize the nanostructures of BHJ blend films [24,64,65]. Referring to the established insights into the P3HT/PC₆₁BM BHJ system [64], the P3HT/PC₆₁BM blend film is generally comprised of three kinds of structures: (1) P3HT crystallites; (2) PC₆₁BM clusters with size of 10–20 nm and (3) meso-scaled domains of amorphous P3HT chains intercalated with PC₆₁BM molecules (denoted as PC₆₁BM/amorphous P3HT). The authors stated that the thermally degraded device performance was actually attributed to the growth and densification of PC₆₁BM/amorphous P3HT domains (structure (3)) instead of the nano-scaled PC₆₁BM clusters (structure (2)) [63]. In other words, the authors clarified the mistaken impression in the developing or coalescing of nano-scaled PC₆₁BM clusters during long-time thermal annealing, which was discovered to be stably confined with unnoticeable change in both size and volume fraction (Figure 7c). Through inter-repulsion of neighboring fullerene cages by stereo-isomers, the additive *bis*-PC₆₁BM can function to suppress the densification of P3HT and PC₆₁BM phases within the PC₆₁BM/amorphous P3HT domains as well as their aggressive growth.

In short, the design of a fullerene derivative for morphological compatibilization/stabilization can be generally directed to a critical guideline: the molecule should be able to anchor the PC₆₁BM molecules through chemical or physical interaction for hindering the thermal-driven diffusion. A more advanced goal is to situate the additives in the amorphous regions to prevent destruction of the donor or acceptor crystalline structure and effectively fixing the PC₆₁BM molecules in amorphous domains.

4. Inorganic Nanocrystals

Inorganic nanocrystals (INCs) can also be included into BHJ film, which is an extensively adopted strategy to enhance device performances [65–69]. The main focus lies on their unique plasma effects for enhancing light scattering path within the thin films. Nonetheless, the incorporation of inorganic materials is never trivial owing to the incompatibility between organic/inorganic hybrid materials. Chemical modification, interface engineering, co-solvent system, *etc.*, can be general strategies to conquer the challenges. Therefore, to date rare reports stating the doping of INCs into organic BHJ films do help the morphologies.

Khan *et al.* reported the *in situ* nanocrystals growth of cadmium telluride in P3HT matrix through dipole-dipole interactions [70]. The methods improved the compatibility between P3HT/CdTe interfaces and prevented the usage of insulating surfactants, which were typically used in INCs synthesis. The embedded CdTe functioned to facilitate the bi-continuous pathways for carrier transport. The P3HT-CdTe/PC₆₁BM ternary blended showed PCE increased by near 10% as compared to the P3HT/PC₆₁BM binary BHJ device.

In our previous work, we successfully doped Cu₂S inorganic nanoparticles (INPs) with diameter of 4–5 nm as morphological control agents [65]. The nano-organized nanostructure of P3HT/PC₆₁BM can be controlled by the INPs with finely tuned concentrations. The quantitative characterization by GISAXS/GIWAXS techniques provided the evidences that the INPs assisted the diffusion of PC₆₁BM to form nano-scaled clusters. Such method imparted similar effect to the traditionally employed thermal annealing for obtaining optimized morphology with proper phase separation. The unique nanoparticle-tuned nanostructure was furthermore discovered to be thermal stable. Such strategy is potentially universal by using a variety of INCs such as CdSe INCs with similar sizes.

5. Summary and Outlook

Incorporating additives has shown to be effective in morphological control and stabilization. Promising candidates for morphological control agents could be polymers, small molecules or inorganic nanocrystals. Optimized morphology can be attained in ternary blend with improved device performance and furthermore be preserved after experiencing harsh environment conditions. Moreover, such strategy benefits the ease of processing and alleviates the complicated encapsulation for withstanding the thermal instability. The ternary blend is thus considered as a feasible direction toward the goal of commercializing OPV. Materials design/synthesis for additives is therefore the most critical subject to realize the effect in real products. It is a case-by-case design depending on a variety of BHJ systems and solvent systems. The present contribution comprehensively reviewed the recent research articles and emphasized on polymers, small molecules (fullerene derivatives) and INCs. The general guidelines are summarized herein which can be served to rationally design the additives toward high efficiency and high stability OPV.

Acknowledgments

The financial support by Ministry of Science and Technology of Taiwan (102-2221-E-002-230-MY3 and 103-3113-E-002-011) was highly appreciated.

Author Contributions

Wei-Fang Su conceived and developed the ideas and contributed to the scientific goals. Po-Hsuen Chen organized the references and re-drew the figures. Hsueh-Chung Liao, Robert P.H. Chang and Wei-Fang Su contributed to the writing of the manuscript.

Conflicts of Interest

The authors declare no conflict of interest.

References

1. Liao, H.C.; Ho, C.C.; Chang, C.Y.; Jao, M.H.; Darling, S.B.; Su, W.F. Additives for morphology control in high-efficiency organic solar cells. *Mater. Today* **2013**, *16*, 326–336.
2. Cheng, Y.J.; Yang, S.H.; Hsu, C.S. Synthesis of conjugated polymers for organic solar cell applications. *Chem. Rev.* **2009**, *109*, 5868–5923.
3. Kozycz, L.M.; Gao, D.; Hollinger, J.; Seferos, D.S. Donor–donor block copolymers for ternary organic solar cells. *Macromolecules* **2012**, *45*, 5823–5832.
4. Bian, L.; Zhu, E.; Tang, J.; Tang, W.; Zhang, F. Recent progress in the design of narrow bandgap conjugated polymers for high-efficiency organic solar cells. *Prog. Polym. Sci.* **2012**, *37*, 1292–1331.
5. Su, Y.W.; Lan, S.C.; Wei, K.H. Organic photovoltaics. *Mater. Today* **2012**, *15*, 554–562.
6. Brabec, C.J.; Heeney, M.; McCulloch, I.; Nelson, J. Influence of blend microstructure on bulk heterojunction organic photovoltaic performance. *Chem. Soc. Rev.* **2011**, *40*, 1185–1199.

7. Chen, W.; Nikiforov, M.P.; Darling, S.B. Morphology characterization in organic and hybrid solar cells. *Energy Environ. Sci.* **2012**, *5*, 8045–8074.
8. Ruderer, M.A.; Müller-Buschbaum, P. Morphology of polymer-based bulk heterojunction films for organic photovoltaics. *Soft Matter* **2011**, *7*, 5482–5493.
9. Brady, M.A.; Su, G.M.; Chabynyc, M.L. Recent progress in the morphology of bulk heterojunction photovoltaics. *Soft Matter* **2011**, *7*, 11065–11077.
10. Liu, F.; Gu, Y.; Jung, J.W.; Jo, W.H.; Russell, T.P. On the morphology of polymer-based photovoltaics. *J. Polym. Sci. B Polym. Phys.* **2012**, *50*, 1018–1044.
11. Janssen, R.A.; Nelson, J. Factors limiting device efficiency in organic photovoltaics. *Adv. Mater.* **2013**, *25*, 1847–1858.
12. Braun, S.; Salaneck, W.R.; Fahlman, M. Energy-level alignment at organic/metal and organic/organic interfaces. *Adv. Mater.* **2009**, *21*, 1450–1472.
13. Deibel, C.; Strobel, T.; Dyakonov, V. Role of the charge transfer state in organic donor-acceptor solar cells. *Adv. Mater.* **2010**, *22*, 4097–4111.
14. Piliago, C.; Loi, M.A. Charge transfer state in highly efficient polymer–fullerene bulk heterojunction solar cells. *J. Mater. Chem.* **2012**, *22*, 4141–4150.
15. Sista, S.; Hong, Z.; Chen, L.M.; Yang, Y. Tandem polymer photovoltaic cells—Current status, challenges and future outlook. *Energy Environ. Sci.* **2011**, *4*, 1606–1620.
16. Ma, W.L.; Yang, C.Y.; Gong, X.; Lee, K.; Heeger, A.J. Thermally stable, efficient polymer solar cells with nanoscale control of the interpenetrating network morphology. *Adv. Funct. Mater.* **2005**, *15*, 1617–1622.
17. Li, G.; Shrotriya, V.; Huang, J.; Yao, Y.; Moriarty, T.; Emery, K.; Yang, Y. High-efficiency solution processable polymer photovoltaic cells by self-organization of polymer blends. *Nat. Mater.* **2005**, *4*, 864–868.
18. Kim, Y.; Cook, S.; Tuladhar, S.M.; Choulis, S.A.; Nelson, J.; Durrant, J.R.; Bradley, D.D.C.; Giles, M.; McCulloch, I.; Ha, C.S.; *et al.* A strong regioregularity effect in self-organizing conjugated polymer films and high-efficiency polythiophene:fullerene solar cells. *Nat. Mater.* **2006**, *5*, 197–203.
19. Yang, X.N.; Loos, J.; Veenstra, S.C.; Verhees, W.J.H.; Wienk, M.M.; Kroon, J.M.; Michels, M.A.J.; Janssen, R.A.J. Nanoscale morphology of high-performance polymer solar cells. *Nano Lett.* **2005**, *5*, 579–583.
20. Li, G.; Yao, Y.; Yang, H.; Shrotriya, V.; Yang, G.; Yang, Y. “Solvent annealing” effect in polymer solar cells based on poly(3-hexylthiophene) and methanofullerenes. *Adv. Funct. Mater.* **2007**, *17*, 1636–1644.
21. Ruderer, M.A.; Guo, S.; Meier, R.; Chiang, H.Y.; Körstgens, V.; Wiedersich, J.; Perlich, J.; Roth, S.V.; Müller-Buschbaum, P. Solvent-induced morphology in polymer-based systems for organic photovoltaics. *Adv. Funct. Mater.* **2011**, *21*, 3382–3391.
22. Peet, J.; Kim, J.Y.; Coates, N.E.; Ma, W.L.; Moses, D.; Heeger, A.J.; Bazan, G.C. Efficiency enhancement in low-bandgap polymer solar cells by processing with alkane dithiols. *Nat. Mater.* **2007**, *6*, 497–500.

23. Dang, M.T.; Hirsch, L.; Wantz, G.; Wuest, J.D. Controlling the morphology and performance of bulk heterojunctions in solar cells. Lessons learned from the benchmark poly(3-hexylthiophene):[6,6]-phenyl-C₆₁-butyric acid methyl ester system. *Chem. Rev.* **2013**, *113*, 3734–3765.
24. Rivnay, J.; Mannsfeld, S.C.; Miller, C.E.; Salleo, A.; Toney, M.F. Quantitative determination of organic semiconductor microstructure from the molecular to device scale. *Chem. Rev.* **2012**, *112*, 5488–5519.
25. Ameri, T.; Khoram, P.; Min, J.; Brabec, C.J. Organic ternary solar cells: A review. *Adv. Mater.* **2013**, *25*, 4245–4266.
26. Chen, Y.C.; Hsu, C.Y.; Lin, R.Y.; Ho, K.C.; Lin, J.T. Materials for the active layer of organic photovoltaics: ternary solar cell approach. *ChemSusChem* **2013**, *6*, 20–35.
27. Yang, L.; Yan, L.; You, W. Organic solar cells beyond one pair of donor–acceptor: Ternary blends and more. *J. Phys. Chem. Lett.* **2013**, *4*, 1802–1810.
28. Meier, R.; Schindler, M.; Muller-Buschbaum, P.; Watts, B. Residual solvent content in conducting polymer-blend films mapped with scanning transmission X-ray microscopy. *Phys. Rev. B* **2011**, *84*, doi:10.1103/PhysRevB.84.174205.
29. Brabec, C.J.; Padinger, F.; Sariciftci, N.S.; Hummelen, J.C. Photovoltaic properties of conjugated polymer/methanofullerene composites embedded in a polystyrene matrix. *J. Appl. Phys.* **1999**, *85*, doi:10.1063/1.370205.
30. Brabec, C.J.; Johansson, H.; Padinger, F.; Neugebauer, H.; Hummelen, J.C.; Sariciftci, N.S. Photoinduced FT-IR spectroscopy and CW-photocurrent measurements of onjugated polymers and fullerenes blended into a conventional polymer matrix. *Sol. Energy Mater. Sol. Cells* **2000**, *61*, 19–33.
31. Camaioni, N.; Catellani, M.; Luzzati, S.; Migliori, A. Morphological characterization of poly(3-octylthiophene):plasticizer:C₆₀ blends. *Thin Solid Films* **2002**, *403–404*, 489–494.
32. Lee, M.; Cho, B.K.; Zin, W.C. Supramolecular structures from rod-coil block copolymers. *Chem. Rev.* **2001**, *101*, 3869–3892.
33. Klok, H.A. Supramolecular materials via block copolymer self-assembly. *Adv. Mater.* **2001**, *13*, 1217–1229.
34. Jenekhe, S.A.; Chen, X.L. Self-assembled aggregates of rod-coil block copolymers and their solubilization and encapsulation of fullerenes. *Science* **1998**, *279*, 1903–1907.
35. Jenekhe, S.A.; Chen, X.L. Self-assembly of ordered microporous materials from rod-coil block copolymers. *Science* **1999**, *283*, 372–375.
36. He, M.; Qiu, F.; Lin, Z. Conjugated rod–coil and rod–rod block copolymers for photovoltaic applications. *J. Mater. Chem.* **2011**, *21*, 17039–17048.
37. Tsai, J.H.; Lai, Y.C.; Higashihara, T.; Lin, C.J.; Ueda, M.; Chen, W.C. Enhancement of P3HT/PCBM photovoltaic efficiency using the surfactant of triblock copolymer containing poly(3-hexylthiophene) and poly(4-vinyltriphenylamine) segments. *Macromolecules* **2010**, *43*, 6085–6091.
38. Sivula, K.; Ball, Z.T.; Watanabe, N.; Fréchet, J.M.J. Amphiphilic diblock copolymer compatibilizers and their effect on the morphology and performance of polythiophene:fullerene solar cells. *Adv. Mater.* **2006**, *18*, 206–210.

39. Yang, C.; Lee, J.K.; Heeger, A.J.; Wudl, F. Well-defined donor–acceptor rod–coil diblock copolymers based on P3HT containing C₆₀: The morphology and role as a surfactant in bulk-heterojunction solar cells. *J. Mater. Chem.* **2009**, *19*, 5416–5423.
40. Lee, J.U.; Jung, J.W.; Emrick, T.; Russell, T.P.; Jo, W.H. Morphology control of a polythiophene–fullerene bulk heterojunction for enhancement of the high-temperature stability of solar cell performance by a new donor-acceptor diblock copolymer. *Nanotechnology* **2010**, *21*, doi:10.1088/0957-4484/21/10/105201.
41. Im, M.J.; Son, S.Y.; Moon, B.J.; Lee, G.Y.; Kim, J.H.; Park, T. Improved photovoltaic performance by enhanced crystallinity of poly(3-hexyl)thiophene. *Org. Electron.* **2013**, *14*, 3046–3051.
42. Mulherin, R.C.; Jung, S.; Huettnner, S.; Johnson, K.; Kohn, P.; Sommer, M.; Allard, S.; Scherf, U.; Greenham, N.C. Ternary photovoltaic blends incorporating an all-conjugated donor-acceptor diblock copolymer. *Nano Lett.* **2011**, *11*, 4846–4851.
43. Rajaram, S.; Armstrong, P.B.; Kim, B.J.; Frechet, J.M.J. Effect of addition of a diblock copolymer on blend morphology and performance of poly(3-hexylthiophene):perylene diimide solar cells. *Chem. Mater.* **2009**, *21*, 1775–1777.
44. Economopoulo, S.P.; Chochos, C.L.; Gregoriou, V.G.; Kallitsis, J.K.; Barrau, S.; Hadziioannou, G. Novel brush-type copolymers bearing thiophene backbone and side chain quinoline blocks. Synthesis and their use as a compatibilizer in thiophene-quinoline polymer blends. *Macromolecules* **2007**, *40*, 921–927.
45. Jung, J.W.; Jo, J.W.; Jo, W.H. Enhanced performance and air stability of polymer solar cells by formation of a self-assembled buffer layer from fullerene-end-capped poly(ethylene glycol). *Adv. Mater.* **2011**, *23*, 1782–1787.
46. Tai, Q.; Li, J.; Liu, Z.; Sun, Z.; Zhao, X.; Yan, F. Enhanced photovoltaic performance of polymer solar cells by adding fullerene end-capped polyethylene glycol. *J. Mater. Chem.* **2011**, *21*, 6848–6853.
47. Lee, J.U.; Jung, J.W.; Emrick, T.; Russell, T.P.; Jo, W.H. Synthesis of C₆₀-end capped P3HT and its application for high performance of P3HT/PCBM bulk heterojunction solar cells. *J. Mater. Chem.* **2010**, *20*, 3287–3294.
48. Chen, J.; Yu, X.; Hong, K.; Messman, J.M.; Pickel, D.L.; Xiao, K.; Dadmun, M.D.; Mays, J.W.; Rondinone, A.J.; Sumpter, B.G.; *et al.* Ternary behavior and systematic nanoscale manipulation of domain structures in P3HT/PCBM/P3HT-b-PEO films. *J. Mater. Chem.* **2012**, *22*, 13013–13022.
49. Sun, Z.; Xiao, K.; Keum, J.K.; Yu, X.; Hong, K.; Browning, J.; Ivanov, I.N.; Chen, J.; Alonzo, J.; Li, D.; *et al.* PS-*b*-P3HT copolymers as P3HT/PCBM interfacial compatibilizers for high efficiency photovoltaics. *Adv. Mater.* **2011**, *23*, 5529–5535.
50. Campoy-Quiles, M.; Kanai, Y.; El-Basaty, A.; Sakai, H.; Murata, H. Ternary mixing: A simple method to tailor the morphology of organic solar cells. *Org. Electron.* **2009**, *10*, 1120–1132.
51. Lee, J.K.; Ma, W.L.; Brabec, C.J.; Yuen, J.; Moon, J.S.; Kim, J.K.; Lee, K.; Bazan, G.C.; Heeger, A.J. Processing additives for improved efficiency from bulk heterojunction solar cells. *J. Am. Chem. Soc.* **2008**, *130*, 3619–3623.
52. Chang, S.Y.; Liao, H.C.; Shao, Y.T.; Sung, Y.M.; Hsu, S.H.; Ho, C.C.; Su, W.F.; Chen, Y.F. Enhancing the efficiency of low bandgap conducting polymer bulk heterojunction solar cells using P3HT as a morphology control agent. *J. Mater. Chem. A* **2013**, *1*, 2447–2452.

53. Kan, Z.; Colella, L.; Canesi, E.V.; Lerario, G.; Kumar, R.S.S.; Bonometti, V.; Mussini, P.R.; Cavallo, G.; Terraneo, G.; Pattanasattayavong, P.; *et al.* Triple bulk heterojunctions as means for recovering the microstructure of photoactive layers in organic solar cell devices. *Sol. Energy Mater. Sol. Cells* **2014**, *120*, 37–47.
54. Cha, H.; Chung, D.S.; Bae, S.Y.; Lee, M.J.; An, T.K.; Hwang, J.; Kim, K.H.; Kim, Y.H.; Choi, D.H.; Park, C.E. Complementary absorbing star-shaped small molecules for the preparation of ternary cascade energy structures in organic photovoltaic cells. *Adv. Funct. Mater.* **2013**, *23*, 1556–1565.
55. Kim, C.S.; Tinker, L.L.; DiSalle, B.F.; Gomez, E.D.; Lee, S.; Bernhard, S.; Loo, Y.L. Altering the thermodynamics of phase separation in inverted bulk-heterojunction organic solar cells. *Adv. Mater.* **2009**, *21*, 3110–3115.
56. Brabec, C.J.; Sariciftic, S.; Hummelen, J.C. Plastic solar cells. *Adv. Funct. Mater.* **2011**, *11*, 15–26.
57. Li, C.Z.; Yip, H.L.; Jen, A.K.Y. Functional fullerenes for organic photovoltaics. *J. Mater. Chem.* **2012**, *22*, 4161–4177.
58. Lai, Y.C.; Higashihara, T.; Hsu, J.C.; Ueda, M.; Chen, W.C. Enhancement of power conversion efficiency and long-term stability of P3HT/PCBM solar cells using C₆₀ derivatives with thiophene units as surfactants. *Sol. Energy Mater. Sol. Cells* **2012**, *97*, 164–170.
59. Cheng, Y.J.; Hsieh, C.H.; Li, P.J.; Hsu, C.S. Morphological stabilization by *in situ* polymerization of fullerene derivatives leading to efficient, thermally stable organic photovoltaics. *Adv. Funct. Mater.* **2011**, *21*, 1723–1732.
60. Liao, M.H.; Tsai, C.E.; Lai, Y.Y.; Cao, F.Y.; Wu, J.S.; Wang, C.L.; Hsu, C.S.; Liao, I.; Cheng, Y.J. Morphological stabilization by supramolecular perfluorophenyl-C₆₀ interactions leading to efficient and thermally stable organic photovoltaics. *Adv. Funct. Mater.* **2014**, *24*, 1418–1429.
61. Liu, H.W.; Chang, D.Y.; Chiu, W.Y.; Rwei, S.P.; Wang, L. Fullerene bisadduct as an effective phase-separation inhibitor in preparing poly(3-hexylthiophene)-[6,6]-phenyl-C₆₁-butyric acid methyl ester blends with highly stable morphology. *J. Mater. Chem.* **2012**, *22*, 15586–15591.
62. Li, F.; Yager, K.G.; Dawson, N.M.; Yang, J.; Malloy, K.J.; Qin, Y. Complementary hydrogen bonding and block copolymer self-assembly in cooperation toward stable solar cells with tunable morphologies. *Macromolecules* **2013**, *46*, 9021–9031.
63. Chen, C.Y.; Tsao, C.S.; Huang, Y.C.; Liu, H.W.; Chiu, W.Y.; Chuang, C.M.; Jeng, U.S.; Su, C.J.; Wu, W.R.; Su, W.F.; *et al.* Mechanism and control of the structural evolution of a polymer solar cell from a bulk heterojunction to a thermally unstable hierarchical structure. *Nanoscale* **2013**, *5*, 7629–7638.
64. Liao, H.C.; Tsao, C.S.; Lin, T.H.; Chuang, C.M.; Chen, C.Y.; Jeng, U.S.; Su, C.H.; Chen, Y.F.; Su, W.F. Quantitative nanoorganized structural evolution for a high efficiency bulk heterojunction polymer solar cell. *J. Am. Chem. Soc.* **2011**, *133*, 13064–13073.
65. Liao, H.C.; Tsao, C.S.; Lin, T.H.; Jao, M.H.; Chuang, C.M.; Chang, S.Y.; Huang, Y.C.; Shao, Y.T.; Chen, C.Y.; Su, C.J.; *et al.* Nanoparticle-tuned self-organization of a bulk heterojunction hybrid solar cell with enhanced performance. *ACS Nano* **2012**, *6*, 1657–1666.

66. Li, X.; Choy, W.C.; Huo, L.; Xie, F.; Sha, W.E.; Ding, B.; Guo, X.; Li, Y.; Hou, J.; You, J.; *et al.* Dual plasmonic nanostructures for high performance inverted organic solar cells. *Adv. Mater.* **2012**, *24*, 3046–3052.
67. Li, X.; Choy, W.C.H.; Lu, H.; Sha, W.E.I.; Ho, A.H.P. Efficiency enhancement of organic solar cells by using shape-dependent broadband plasmonic absorption in metallic nanoparticles. *Adv. Funct. Mater.* **2013**, *23*, 2728–2735.
68. Chen, H.C.; Chou, S.W.; Tseng, W.H.; Chen, I.W.P.; Liu, C.C.; Liu, C.; Liu, C.L.; Chen, C.H.; Wu, C.I.; Chou, P.T. Large AuAg alloy nanoparticles synthesized in organic media using a one-pot reaction: Their applications for high-performance bulk heterojunction solar cells. *Adv. Funct. Mater.* **2012**, *22*, 3975–3984.
69. Wang, D.H.; Kim, D.Y.; Choi, K.W.; Seo, J.H.; Im, S.H.; Park, J.H.; Park, O.O.; Heeger, A.J. Enhancement of donor–acceptor polymer bulk heterojunction solar cell power conversion efficiencies by addition of Au nanoparticles. *Angew. Chem.* **2011**, *50*, 5519–5523.
70. Taukeer Khan, M.; Kaur, A.; Dhawan, S.K.; Chand, S. *In-situ* growth of cadmium telluride nanocrystals in poly(3-hexylthiophene) matrix for photovoltaic application. *J. Appl. Phys.* **2011**, *110*, doi:10.1063/1.3626464.

© 2014 by the authors; licensee MDPI, Basel, Switzerland. This article is an open access article distributed under the terms and conditions of the Creative Commons Attribution license (<http://creativecommons.org/licenses/by/4.0/>).